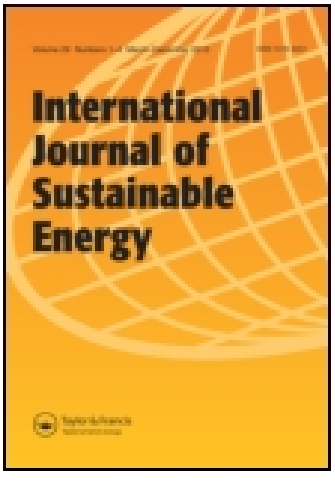

International Journal of Sustainable Energy

Publication details, including instructions for authors and subscription information:
http://www.tandfonline.com/loi/gsol20

Energy flow and management of a hybrid wind/PV/fuel cell generation system

Thanaa F. El-Shater [a] , Mona N. Eskander [a] & Mohsen T. El-Hagry [a]

[a] Electronics Research Institute , National Research Center, Tahrir Street, Dokki , Cairo, Egypt

Published online: 11 Oct 2011.

To cite this article: Thanaa F. El-Shater , Mona N. Eskander & Mohsen T. El-Hagry (2006) Energy flow and management of a hybrid wind/PV/fuel cell generation system, International Journal of Sustainable Energy, 25:2, 91-106, DOI: 10.1080/14786450600631483

To link to this article: http://dx.doi.org/10.1080/14786450600631483

International Journal of Sustainable Energy
Vol. 25, No. 2, June 2006, 91–106

Taylor & Francis
Taylor & Francis Group

Energy flow and management of a hybrid wind/PV/fuel cell generation system

THANAA F. EL-SHATER*, MONA N. ESKANDER and MOHSEN T. EL-HAGRY

Electronics Research Institute, National Research Center, Tahrir Street, Dokki, Cairo, Egypt

In this paper, an energy system comprising three energy sources, namely PV, wind, and fuel cells (FCs), is proposed. Each of the three energy sources is controlled so as to deliver energy at optimum efficiency. Fuzzy logic control is employed to achieve maximum power tracking for both PV and wind energies and to deliver this maximum power to a fixed DC voltage bus. The fixed voltage bus supplies the load while the excess power feeds the water electrolyzer used to generate hydrogen for supplying the FCs. A management system is designed to manage the power flow between the system components in order to satisfy the load requirements throughout the whole day. A case study is carried out using practical data from a site at El-Hammam (40 km west of Alexandria, Egypt). The study defines the power generated by wind and PV systems, the hydrogen generated using and stored in tanks, and the power generated by the FCs to supply the deficiency in the load demand. Simulation results, done for two seasons, proved the accuracy of the fuzzy logic controllers. Also, a complete description of the management system is presented.

Keywords:

1. Introduction

Global environmental concerns and the ever-increasing need for energy, coupled with a steady progress in renewable energy technologies, are opening up new opportunities for utilization of renewable energy resources. In particular, advances in wind and PV energy technologies have increased their use in hybrid wind/PV configurations. Integrating PV and wind-energy sources with fuel cells (FCs), as a storage device replacing the conventional lead-acid batteries, leads to a non-polluting reliable energy source. The FC generation system offers many advantages over other generation systems: low pollution, high efficiency, diversity of fuels, reusability of exhaust heat, and on-site installation.

In this paper, a 4.5 kW peak, stand-alone hybrid wind–PV–FC energy system for supplying a 72 V DC voltage load is designed. The system incorporates a water electrolyzer and storage tank to supply the FC stack with hydrogen. The DC power required for hydrogen generation is supplied through the DC bus during surplus PV/wind power. The generated hydrogen is stored in tanks to be utilized by the FCs when the PV and wind-energy sources fail to supply the load demand.

*Corresponding author. Email: thanaa@eri.sci.eg

International Journal of Sustainable Energy
ISSN 1478-6451 print/ISSN 1478-646X online © 2006 Taylor & Francis
http://www.tandf.co.uk/journals
DOI: 10.1080/14786450600631483

The wind-energy conversion system (WECS) incorporated in the proposed scheme consists of a wind turbine (WT) coupled to a permanent magnet synchronous generator. An AC–DC power electronic interface with diode bridge rectifier and two DC–DC buck-boost converters are used for maximum power tracking (MPT) and DC output voltage regulation. Two fuzzy logic controllers (FLCs) are designed to adjust the duty cycles of the two buck-boost converters to achieve MPT and output voltage regulation. This scheme differs from previous schemes (Simoes *et al.* 1997, Ferrao *et al.* 1999), in that simultaneous MPT and voltage regulation are attained, and a different control algorithm is proposed.

The photovoltaic (PV) array interconnected with the proposed scheme consists of 40 polycrystalline silicon solar cells modules, which each deliver 56 W peak. Two DC–DC buck-boost converters are used to deliver the maximum power point (MPP) and DC output voltage regulation. The MPP are determined online using the fuzzy regression model (FRM) (El-Shater 1998). The MPP and output voltage regulation are achieved through the application of the FLC.

The flow of energy is managed throughout the proposed system to assure continuous supply of the load demand. The main objective of the power management system is to supply the load with its full demand while monitoring the pressure in the hydrogen tank (hydrogen threshold pressure 'PTH'). This aim is achieved through the following steps.

1. Monitoring the state of the stored hydrogen, as well as that of the wind and solar power generated and comparing them with the load demand.
2. Issue commands to the FCs control valves and the control circuits to control the power flow to the load.
3. Issue commands to operate the electrolyzer in order to use the excess energy to generate hydrogen for future use, *i.e.* when needed.

2. System description

The proposed system is composed of the following subsystems:

1. A 2.25 kW wind-energy conversion system with FLCs.
2. A 2.24 kW PV array subsystem.
3. An electrolyzer for hydrogen generation when the generated power exceeds the load demand.
4. Hydrogen storage tank.
5. FCs stack to supply load when wind/PV system generated power is insufficient.
6. Load.
7. Managing system incorporating valves and switches controlled digitally to achieve continuous supply of load demand.

2.1 *Wind-energy conversion subsystem (WECS)*

The block diagram of the wind-energy system (WES) adopted in this paper is shown in figure 1. It consists of a horizontal axis WT coupled to a permanent magnet synchronous generator. An AC–DC power electronic interface with diode bridge rectifier and two DC–DC buck-boost converters are used to track and extract maximum power available from the WES for a given wind velocity and deliver this power to a 72 V DC constant voltage load. The system is designed to achieve MPT and output voltage regulation within a wide range of wind speed variation (3–8 m/s) by means of two FLCs. The first FLC is designed to vary the on-time 'd_1' of the switching device of the first buck-boost converter (BB1) as wind speed changes, in order to

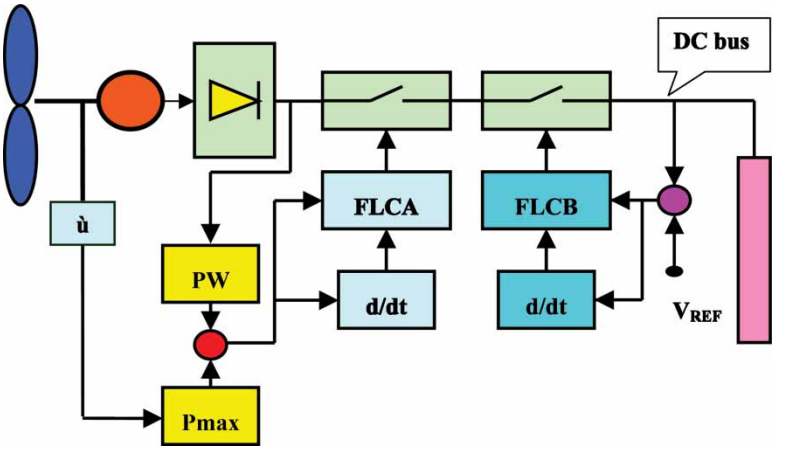

Figure 1. Schematic of WECS with FLC.

achieve MPT within the considered wind speeds range. The second FLC is designed to output the on-time 'd_2' of the switching device of the second buck-boost converter (BB2) to achieve output voltage regulation within the same wind speed range. The subsystems modeling are described as follows:

2.1.1 Wind turbine. The power captured by the WT is calculated as

$$P_{\mathrm{w}} = 0.5 C_{\mathrm{p}} \rho \pi R^2 V_{\mathrm{w}}^3 \tag{1}$$

where V_{w} is the average wind velocity (m/s), ρ is the air density (kg/m^3), R is the radius of turbine blades (m), and C_{p} is the power coefficient, which is a function of the tip speed ratio λ given by

$$\lambda = \omega_{\mathrm{m}} R / V_{\mathrm{w}} \tag{2}$$

where ω_{m} is the rotor mechanical speed (rad/s).

To make an optimal use of the available wind power, it is necessary to change the rotor speed ω_{m} in proportion to the wind speed V_{w} to hold the value for maximum C_{p} as the wind speed varies. The maximum power output from the WES at different rotational turbine speed ω_{m} is computed for the considered WT (Leuven 1982), and the data obtained is used to relate the maximum output power $P_{\max}$ to ω_{m} using polynomial curve fit as shown below.

$$P_{\max} = 0.0005\omega_{\mathrm{m}}^3 - 0.00125\omega_{\mathrm{m}}^2 + 0.7\omega_{\mathrm{m}} - 74.6\,\mathrm{W}. \tag{3}$$

2.1.2 Permanent magnet synchronous generator. A 2.25 kW, 24 pole, 500 rpm rated speed permanent magnet generator (PMG) is employed in the WECS. The generator output voltage varies according to the wind speed variation. Hence, the three-phase output of the PMG is rectified with a full wave diode bridge rectifier, filtered to remove significant ripple voltage components, and fed to two consecutive DC–DC buck-boost converters. For an ideal PMG, the line-to-line voltage is given as (Ryan and Larenz 1997)

$$V_{\mathrm{L}} = K_{\mathrm{v}} \omega_{\mathrm{e}} \sin \omega_{\mathrm{e}} t\,(\mathrm{V}) \tag{4}$$

where K_v is the voltage constant and ω_e is the electrical frequency related to the mechanical speed ω_m by

$$\omega_e = \omega_m \left(\frac{n_p}{2}\right) \text{(rad/s)} \tag{5}$$

where n_p is the number of poles of PMG.

Neglecting commutation delays, the DC rectifier voltage V_d is given as

$$V_d = \left(\frac{3\sqrt{2}}{\pi}\right) V_{Lrms} - \left(\frac{3\omega_e L_s}{\pi}\right) I_d \text{ (V)} \tag{6}$$

where V_{Lrms} is the rms value of the PMG output voltage, I_d is the rectifier output current, and L_s is the stator inductance. Neglecting the generator and rectifier losses, the PMG output rectified electrical power P_{DC} is equal to the mechanical power input to it

$$P_{DC} = V_d I_d \tag{7}$$

2.1.3 Buck-boost converters. The two nonlinear state-space-averaged equations describing the buck-boost converters shown in figure 2 are (Lee 1993)

$$pX_1 = \frac{1-d}{L(X_2)} + \frac{d}{LU} \tag{8}$$

$$pX_2 = -\frac{1-d}{C(X_1)} - \frac{X_2}{RC} \tag{9}$$

where d is the on-time of the switching device, U is the input voltage, X_1 is the inductor current, and X_2 is the output voltage.

2.1.4 FLCs for WECS. Owing to the nonlinearity of the buck-boost converters, FLCs are applied for MPT and output voltage regulation providing two advantages, namely simple and robust nonlinear control systems owning features that cannot be obtained with linear controllers, and by linguistic description for the global behavior of the controllers, the need for a detailed model of the controlled system is avoided.

Two FLCs are designed to achieve the following goals for the WECS.

1. FLC1 varying the on-time (d_1) of the switching device of the first buck-boost converter (BB1) for maximum wind power tracking. The inputs to FLC1 are chosen to be the error

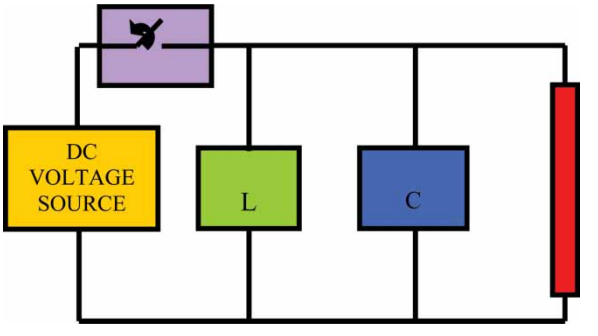

Figure 2. Buck-boost converter circuit.

Table 1. Linguistic control rules relating the inputs and output of the FL controller.

	Cerror				
Error	NG	NS	ZE	PS	PG
NG	NS	ZE	PG	PG	PG
NM	NM	NS	PM	PG	PG
NS	NM	ZE	PS	PM	PM
ZE	NS	NS	ZE	PS	PS
PS	NM	NM	NS	ZE	PM
PM	NG	NS	NM	PS	PM
PG	NS	NG	NG	ZE	PS

between the rectified actual generator power P_w and the maximum available wind power P_{max}, which is defined as 'err' and the change in this error 'cerr'. FLC1 output is the value of d_1.

2. FLC2 varying the on-time (d_2) of the switching device of the second buck-boost converter (BB2) for regulating the output voltage of the WECS. The inputs to FLC2 are chosen to be the error between the reference voltage and the actual output voltage (err) and the change in this error (cerr). FLC2 output is the value of d_2.

Seven uniformly distributed triangular membership functions are used for the 'err' input, whereas five uniformly distributed triangular membership functions are used for both the 'cerr' and outputs for the two FL controllers. The membership functions are denoted by NG (negative large), NM (negative medium), NS (negative small), ZE (zero), PS (positive small), PM (positive medium), and PG (positive large). The linguistic control rules relating the inputs and output of the FL controller are shown in table 1. This rule base is designed such that when the error and change in error are zero, the fuzzy controller has reached the target (maximum power or regulated voltage) and is holding at it. If any disturbance occurs, the rules change to follow the maximum power and voltage reference, according to which converter is controlled.

Figure 3 shows the wind profile within 24 h in summer at the El-Hammam site together with the output power obtained using FLC1. Figure 4 shows the wind profile within 24 h in winter

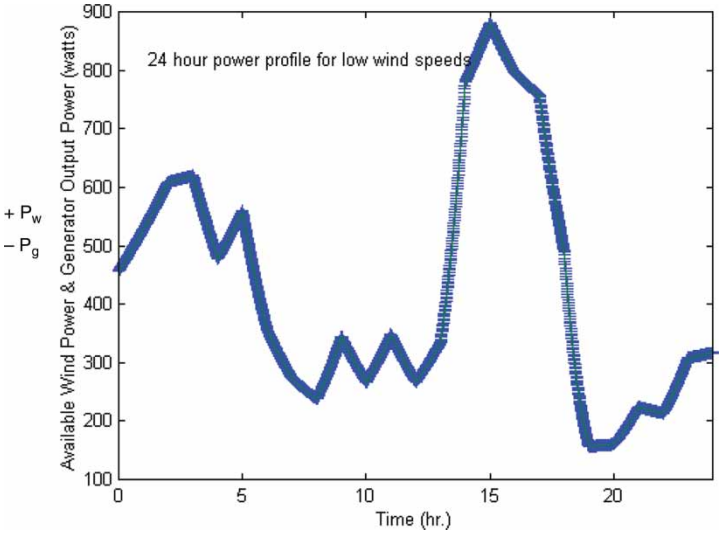

Figure 3. MPT for lower wind speed profile.

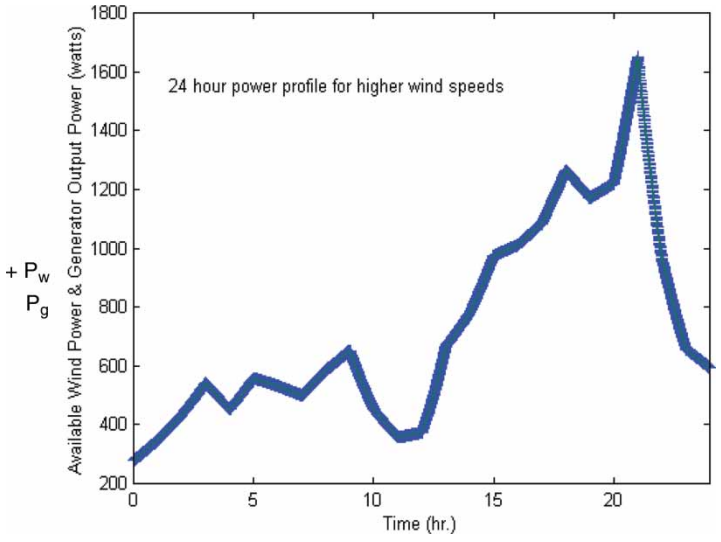

Figure 4. MPT for higher wind speed profile.

at the El-Hammam site together with the output power obtained using FLC1. It is clear in both the cases that the curves of maximum available wind power coincide with the generator output power, which proves that the controller forces the system to extract the maximum power and deliver it as useful electric energy. Figure 5 shows the output DC voltage of BB2 when a step change of 7 V in the reference voltage is applied. It is clear that the output voltage follows the reference value, *i.e.* accurate tracking of the output voltage is achieved via FLC2. The corresponding values of d_1 and d_2 for MPT and output voltage regulation in winter are shown in figures 6 and 7, respectively.

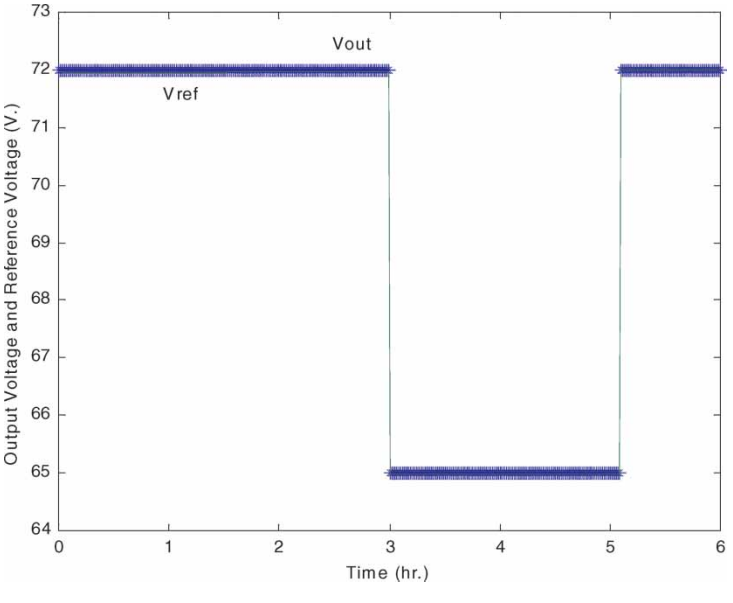

Figure 5. FLC2 tracking at step change in reference voltage.

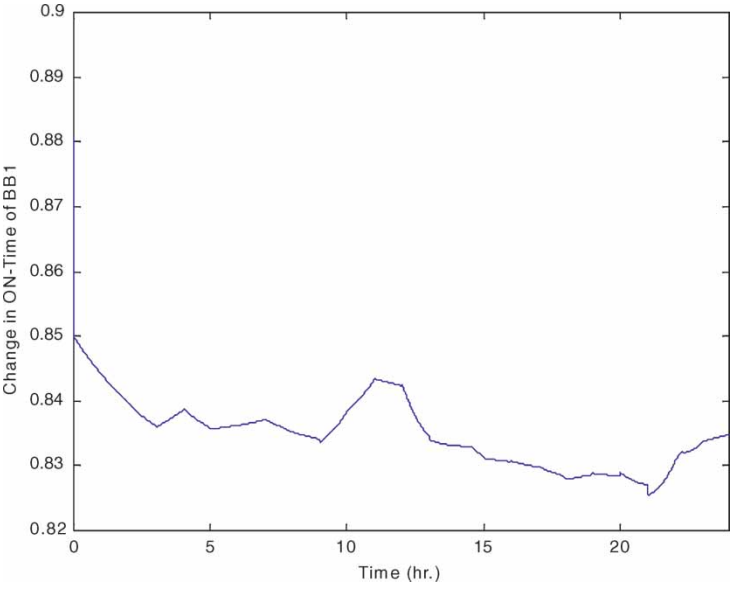

Figure 6. On-time of first buck-boost converter for high wind speeds.

2.2 *PV subsystem*

Figure 8 shows the block diagram of the PV subsystem proposed in this paper. The PV array used consists of 40 modules, each of them deliver 56 W peak (17.7 V and 3.16 A at STC). To satisfy the required load of 72 bus voltage, four of the modules are connected in series and 10 in parallel to obtain the 2.24 kW peak.

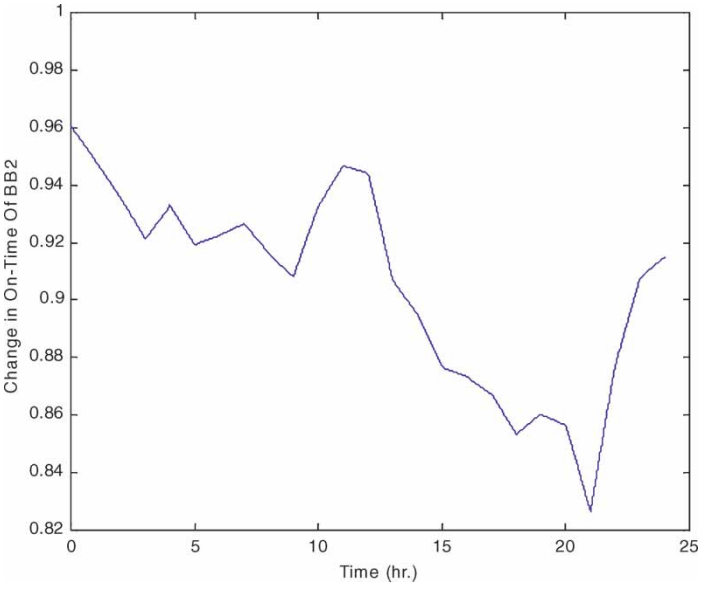

Figure 7. On-time of second buck-boost converter for high wind speeds.

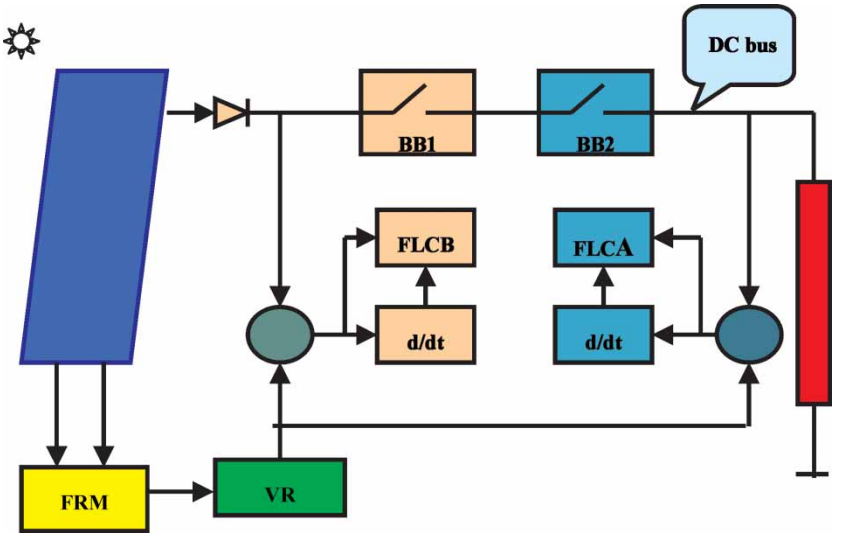

Figure 8. Block diagram of the PV subsystem.

2.2.1 MPP determination To maximize the power extracted from the PV system, the MPP voltage V_{m} and current I_{m} are determined online using FRM (El-Shatter 1998). The FRM is based on the linear possibility system using symmetrical fuzzy number $A_i = (\alpha_i, c_i)$, where α_i is the center and c_i is the width of the reference function $L(x)$ which is expressed as

$$Y = A_0 + A_1 X_1 + A_2 X_2 + \cdots + A_n X_n \tag{10}$$

where A_o is a fuzzy constant, X is the input variables system, and Y is the system output. For both models of V_{m} and I_{m} determination, the fuzzy model input parameters are the solar insolation incident on the array surface W and the panel surface temperature T.

2.2.2 Buck-boost converters. The same type of converters as illustrated in section (2.1.3) are also used in the PV subsystem for power control. Two DC–DC buck-boost converters are used. The first one is used to achieve the MPP (their parameters are denoted with A). The second is used to supply 72 V DC load voltage (their parameters are denoted with B).

2.2.3 FLC for PV subsystem. Owing to the nonlinearity of the PV solar cells, nondeterministic solar cell parameters, and shortage of the available manufacturer data about the system, the application of the FLC is necessary. Two FLCs are designed to achieve the following goals for the PV subsystem.

1. FLCA varying the on-time (d_{A}) of the switching device of the first buck-boost converter (BBA) for MPP tracking. The inputs to FLCA are chosen to be the error between the PV generator power and the determined MPP through the application of the FRM, and defined as 'error', and the change in this error 'cerror'. FLCA output is the new value of d_{A}.

Table 2. PV FLC rules.

	Error						
Cerror	NB	NM	NS	Z	PS	PM	PB
NB	NB	NB	NB	NS	PS	PS	PM
NM	NB	NB	NB	NS	PS	PS	PM
NS	NB	NB	NS	NS	PS	PS	PM
Z	NB	NM	NS	Z	PS	PM	PB
PS	NM	NS	NS	PS	PM	PM	PB
PM	NM	NS	NS	PS	PM	PM	PB
PB	NM	NS	NS	PS	PB	PM	PB

2. FLCB varying the on-time (d_B) of the switching device of the second buck-boost converter (BBB) for regulating the output voltage of the PV subsystem. The inputs to FLCB are chosen to be the error between the reference voltage and the actual output voltage from the first converter (error) and the change in this error (cerror). FLCB output is the new value of d_B.

Seven uniformly distributed triangular membership functions are used for the 'error', 'cerror' inputs, and the output from both FLC. The membership functions are denoted by NB (negative big), NM (negative medium), NS (negative small), Z (zero), PS (positive small), PM (positive medium), and PB (positive big). The linguistic control rules relating the inputs and output of the FLC are shown in table 2. Figures 9 and 10 show the solar insolation measurements at the El-Hammam site during the two seasons (summer and winter, respectively) of 1996. These two extremes are used to test our FLC system and the desired requirements of the MPP tracking for the first converter BBA and the DC bus voltage for the second one (BBB). Figures 9 and 10 show good traceability of the MPP with varying insolation during the day and also with changes in the insolation levels. Figure 11 shows the on-time of the BBA for low insolation level (winter season). Figure 12 shows the 10 V step-down change in the reference signal during a period from 8:00 to 11:00 (3 h), the output voltage from the BBB,

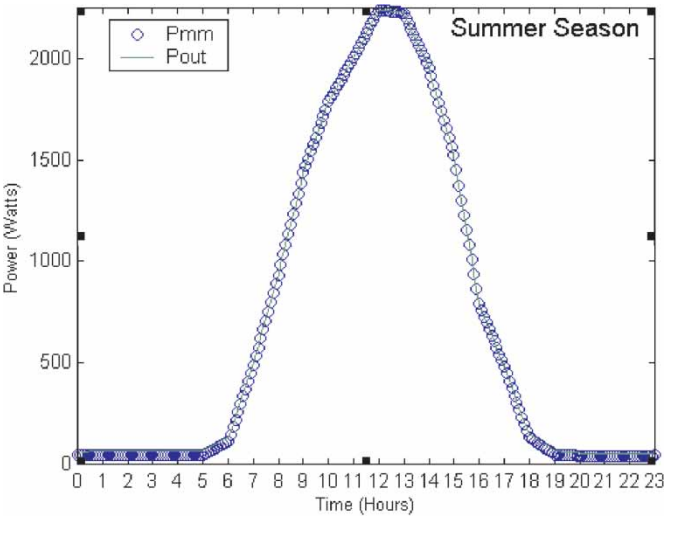

Figure 9. MPP and output power from BBA during summer.

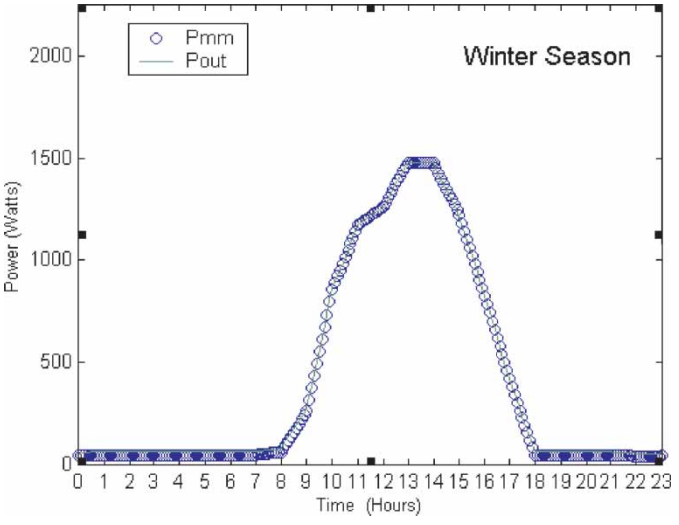

Figure 10. MPP and output power from BBA during winter.

and the corresponding d_B. As shown, an accurate output voltage tracking is achieved via the FLCB.

2.3 *Electrolyzer subsystem*

The unipolar Stuart cell is a high efficiency, low maintenance, rugged and reliable cell. Each electrode has a single polarity producing either H_2 (cathode) or O_2 (anode). The electrolyzer consists of a number of cells isolated from one another in separate cell compartments. Cell voltage under normal operating conditions is in the range of 1.7–1.9 VDC

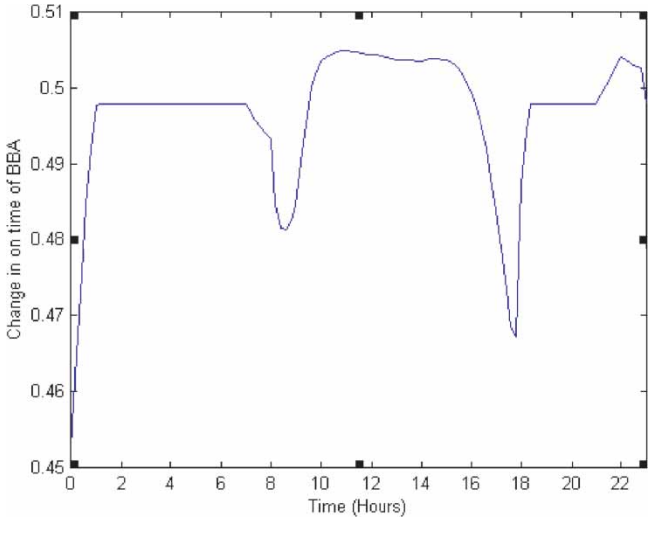

Figure 11. On-time of the BBA for low insolation level.

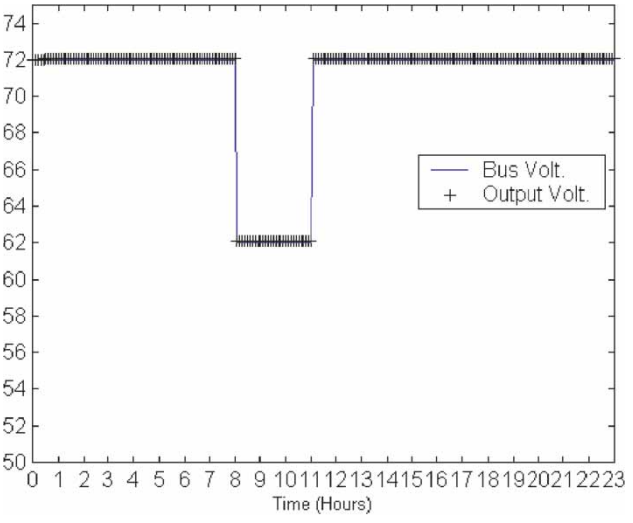

Figure 12. FLCB tracking at step change in reference voltage.

(El-Shater *et al.* 2001). Generated hydrogen is stored in a tank. Inlet and outlet of tank are controlled via the management system, which monitors the hydrogen pressure as well.

2.4 *FC subsystem*

Proton exchange membrane (PEM) FCs stack is used. The PEM uses a polymer membrane as its electrolyte (El-Shater *et al.* 2001).

In the proposed system, air is used as the oxidant; cell pressure is atmospheric and cell temperature 70 °C. Current density is designed as 400 mA/cm^2. This leads to use 576 FCs in stack.

3. System management

3.1 *Management algorithm*

The data from the El-Hammam site on the North Coast is used in the case study. The data include wind speeds, wind direction, solar insolation, and temperature throughout the year. The total wind and solar energy generated simultaneously are calculated and plotted in figure 13 for the winter season. On the same plot, the load power demand is drawn. Figure 14 plots the duty factor D following the available wind and solar generation. D takes the value 1 when the load demand is higher than the total generation and takes values less than 1 when the load demand is less than the total generation. This is clear when relating figures 13 and 14 to each other.

Knowing the load demand, the surplus energy is concluded. Surplus energy is used to generate hydrogen from the electrolyzer and store it in tanks. At times when both wind and PV sources are unable to supply the load demand, the stored hydrogen is supplied to the FCs. The managing system controls the operation of the FC modules to supply deficiency in the load demand. Load shedding is allowed if total power generated is less than load demand.

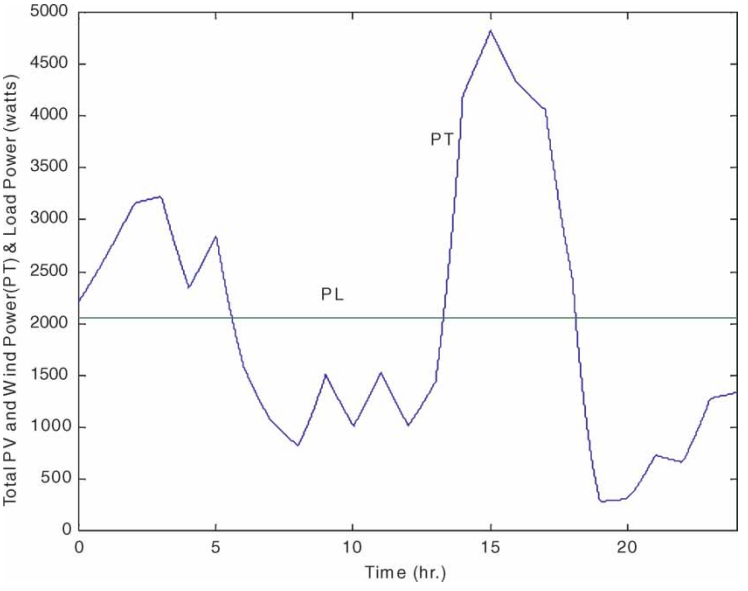

Figure 13. Renewable sources power PT and load power PL.

The FC module is shown in figure 15. The FC module comprises four FC units, namely A1, A2, A3, and A4. The module is designed such that A1 can supply 50% of the load demand, A2 can supply 25% of load demand, while each of A3 and A4 can supply 12.5% of load demand. Hence, the FC module can supply the full load in case of complete shortage of the renewable energy supply. In this figure, V_{1H} to V_{4H} are the valves controlling the hydrogen flow to the

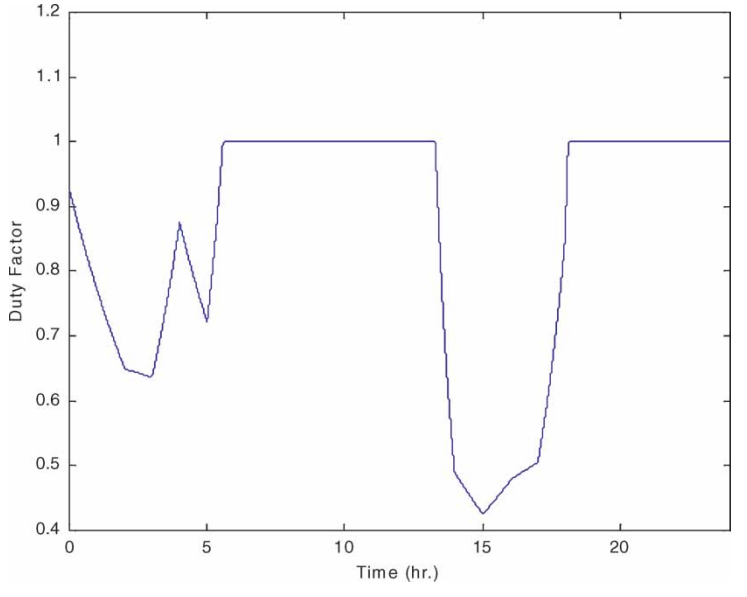

Figure 14. Duty factor.

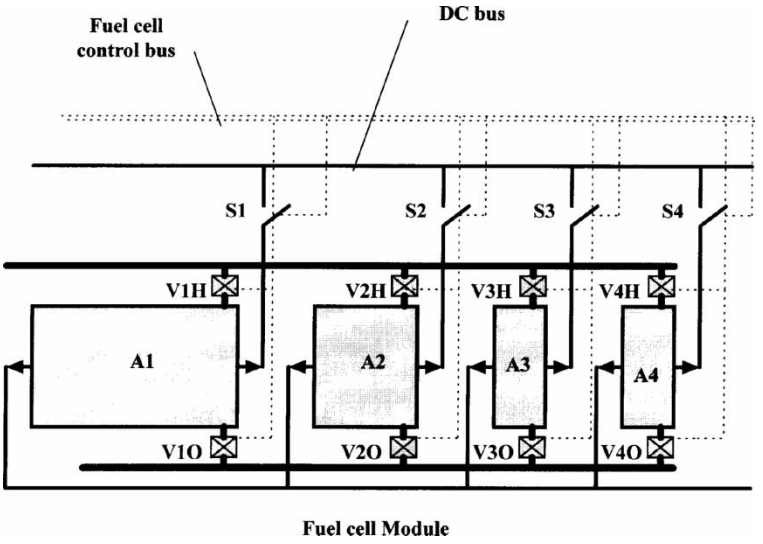

Figure 15. FCs module.

FC and are controlled by the FC control bus. V_{1O} to V_{4O} are the valves controlling the oxygen flow to the FCs and are controlled by the FC control bus. S_1 to S_4 are switches connecting the FC current to the DC bus and are also controlled by FC control bus. Figure 16 demonstrates the role of the management module in controlling the flow of power from the PV, wind, and FC subsystems to the load. The management module monitors the PV power, wind power, load power, and hydrogen tank pressure and issues commands determining the duty factor as well as the states of the different valves and switches of the FC module shown in figure 15. The flow chart describing the management of the power flow in the proposed system is shown in figure 17.

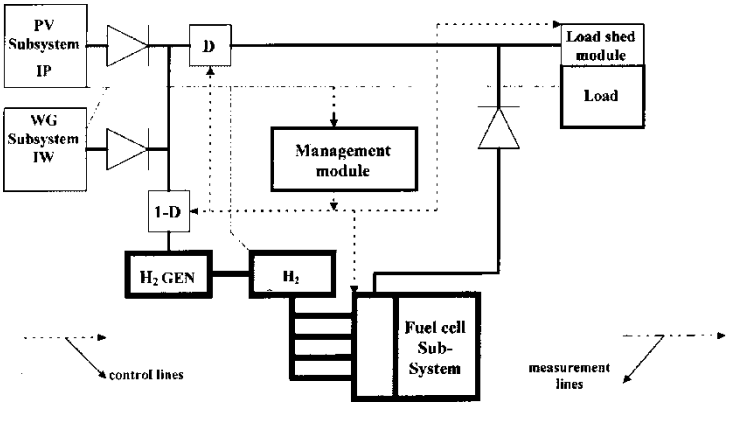

Figure 16. Generation system layout.

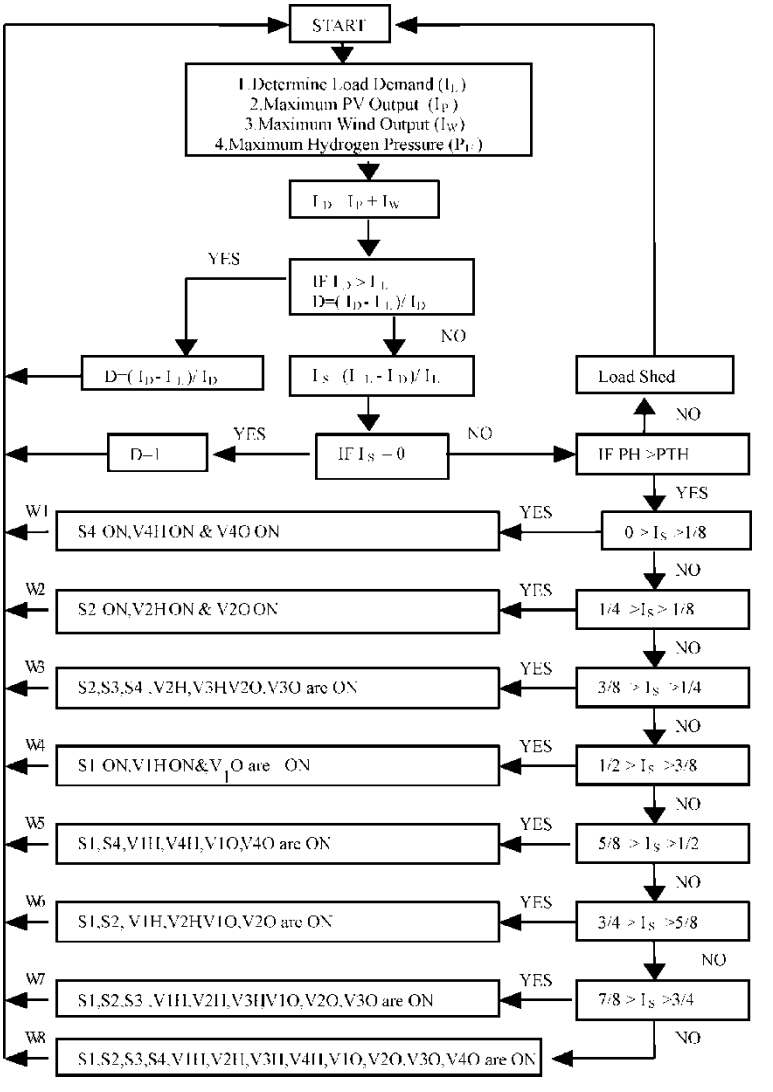

Figure 17. Flow chart of system management.

3.2 *Simulation results*

Simulation results showing the states of the different switches are shown in figure 18 for data taken on 1996 on the El-Hammam site. The results are shown as

$$W_i = [V_{i\mathrm{H}}, V_{i\mathrm{O}}, S_i]$$

where $i = 1, 2, \ldots, 8$ are the states of the management system described in the flow chart. Valves and switches control is achieved via comparator circuits and are activated simultaneously.

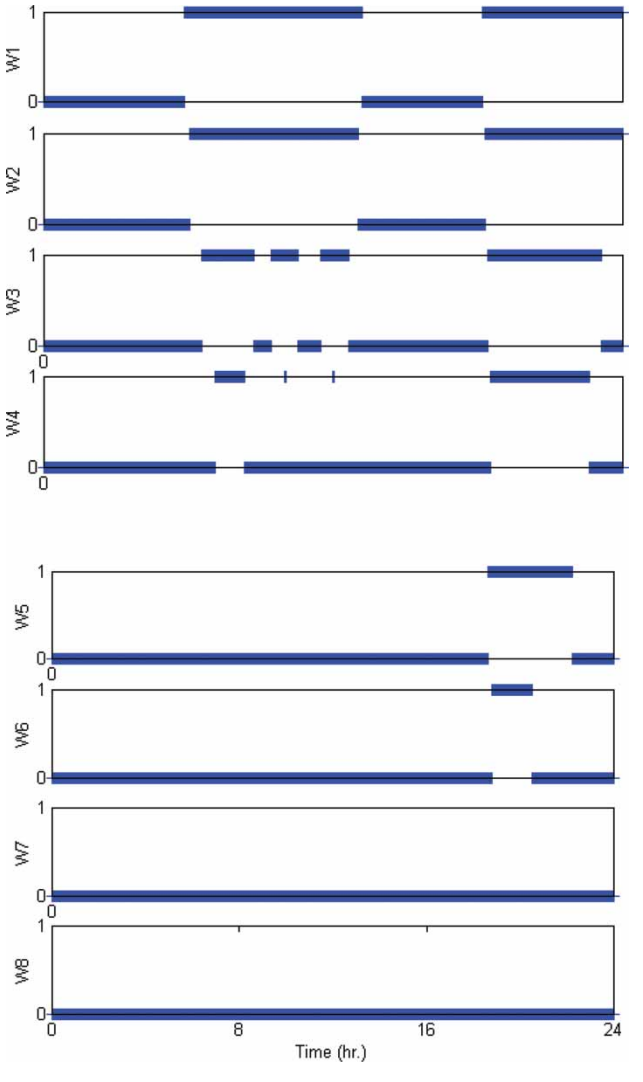

Figure 18. Status of valves and switches for 24 h in January.

4. Conclusion

In this paper, an energy system comprising three energy sources, namely PV, wind, and FCs, is proposed. Each of the three energy sources is controlled so as to deliver energy at optimum efficiency. Fuzzy logic control is employed to achieve MPT for both PV and wind energies and to deliver this maximum power to a fixed DC voltage bus. The results obtained from the research work are as follows:

1. The feasibility of the FLCs for tracking the maximum power available in both wind and PV energy systems.
2. The accuracy of the FLCs in regulating the DC bus voltage at the whole range of wind speeds and solar insolation obtained from the considered site data is proved. This is done

by studying the change in output voltage following an abrupt change in wind speed and/or solar insolation in the presence of the controllers.

3. The proposed system for managing the flow of power is simulated using El-Hammam on-site data. The data include wind speed and PV insolation.

References

Simoes, M.G., Bose, B.K. and Spiegel, R., Fuzzy logic based intelligent control of a variable speed cage machine wind generation system, *IEEE Trans. PE*, 1997, **12**(1), 87–94.

Fernao, V., Amaral, T., Fernando, J. and Crisostomo, M., Fuzzy logic control of a single phase AC/DC buck-boost converter, *Proceedings of EPE Conference*, Switzerland, 1999, 1–10.

El-Shater, T., Fuzzy modeling and simulation of photovoltaic systems, PhD thesis. Cairo University, Faculty of Engineering, 1998.

Leuven, K.U., *Wind Energy for the Eighties*, 1982 (Peter Peregrinus Ltd.: Stevenage, UK).

Ryan, M.J. and Lorenz, R.D., A novel control-oriented model of a PM generator with diode bridge output, in *Proceedings of EPE Conference*, Trondheim, Norway, 1997, 324–329.

Lee, Y.-S. *Computer Aided Analysis and Design of Switch Mode Power Supplies*, 1993 (Marcel Dekker Inc.: New York).

El-Shater, T., Eskander, M. and El-Hagry, M., Hybrid PV/fuel cell system design and simulation, in *36th Intersociety Energy Conversion Engineering Conference*, Savannah, Georgia, 29 July–2 August 2001.